Compression stiffening in biological tissues: On the possibility of classic elasticity origins

T. A. Engstrom,[1,*] K. Pogoda,[2,3] K. Cruz,[2] P. A. Janmey,[2,4,†] and J. M. Schwarz[1,‡]
[1]*Department of Physics, Syracuse University, Syracuse, New York 13244, USA*
[2]*Institute for Medicine and Engineering, The University of Pennsylvania, Philadelphia, Pennsylvania 19104, USA*
[3]*Institute of Nuclear Physics, Polish Academy of Sciences PL-31342, Krakow, Poland*
[4]*Departments of Physiology and Physics & Astronomy, The University of Pennsylvania, Philadelphia, Pennsylvania 19104, USA*

(Received 8 February 2019; published 28 May 2019)

Compression stiffening, or an increase in shear modulus with increasing compressive strain, has been observed in recent rheometry experiments on brain, liver, and fat tissues. Here we extend the known types of biomaterials exhibiting this phenomenon to include agarose gel and fruit flesh. The data reveal a linear relationship between shear storage modulus and uniaxial prestress, even up to 40% strain in some cases. We focus on this less-familiar linear relationship to show that two different results from classic elasticity theory can account for the phenomenon of linear compression stiffening. One result is due to Barron and Klein, extended here to the relevant geometry and prestresses; the other is due to Birch. For incompressible materials, there are no adjustable parameters in either theory. Which one applies to a given situation is a matter of reference state, suggesting that the reference state is determined by the tendency of the material to develop, or not develop, axial stress (in excess of the applied prestress) when subjected to torsion at constant axial strain. Our experiments and analysis also strengthen the notion that seemingly distinct animal and plant tissues can have mechanically similar behavior at the quantitative level under certain conditions.

DOI: 10.1103/PhysRevE.99.052413

I. INTRODUCTION

The effect of prestress on a biological tissue's elastic moduli and related sound velocities, etc., is an interesting question, given that a living tissue confined in volume generically develops prestress in the form of homeostatic pressure. This condition is characterized by a steady state of cell division and death processes [1]. For vascularized tissue, an upper limit on homeostatic pressure is set by the ∼10-kPa blood pressure. *Ex vivo* shear stiffness of mammalian brain matter is ∼1 kPa for comparison [2,3]. One might naturally ask how, or whether, the latter value would be different in the case of living or otherwise prestressed tissue. Very recent results using magnetic resonance elastography indicate the shear modulus of living brain tissue increases linearly with intracranial (homeostatic) pressure [4].

A series of recent parallel-plate rheometry experiments have explored prestress effects in animal tissue and biopolymer network samples of characteristic size ∼1 cm by subjecting them to a combination of static axial compression and ∼1-Hz torsional oscillations [5–10]. To avoid slippage during torsion, and also to facilitate axial tension, adhesive contact is typically made between the rheometer plates and the ends of the cylindrical sample [11]. It has been pointed out that such adhesive boundary conditions effectively constrain the lateral dimensions of a sufficiently thin sample, resulting in a volume change when axial force is applied [8,9]. In this thin-film limit, one expects stresses within a fluid-containing tissue sample are redistributed into a state of near hydrostatic pressure. Thus, by adjusting the sample geometry and/or boundary conditions, parallel-plate rheometers provide a convenient way to measure the effect of various states of prestress on the shear storage and loss moduli of tissues.

These recent experiments have studied, in particular, the shear response of brain tissue (both normal and that isolated from human glioma tumors), as a function of prestress levels expected *in vivo* from homeostatic pressure considerations, as well as increased vascularization of the tumors [5]. Similar measurements were also carried out on liver tissue (both normal and that affected by fibrosis) [6]. In all four of these cases, shear storage modulus is reported to increase with applied uniaxial compression. The authors refer to this phenomenon as *compression stiffening*. Interestingly, when essentially the same experiment is done with the biopolymer network materials collagen and fibrin (major components of the extracellular matrix), the opposite effect is found: Shear storage modulus decreases with uniaxial compression, otherwise known as compression softening, but increases with extension [7,8].

One potentially unifying feature of the diffferent tissue results, however, is an observed linear relationship between shear storage modulus and uniaxial prestress [6,8]. This specific linear relationship has yet to be a focus of modelers. And yet it is this very relationship that clues us in on several potential new mechanisms for compressional stiffening depending on the slope, as we will detail below. And while some of the deformations involved in these experiments are typically what

*tyler.engstrom@gmail.com
†janmey@mail.med.upenn.edu
‡jschwarz@physics.syr.edu

one would consider to be well outside the regime of linear elasticity—on the order of 40% strain or more—the compression stiffening behavior also shows up in (and is qualitatively similar in) the small deformation regime where strains are less than ∼10%. This point is not addressed in prior theoretical work, which focuses on explaining compression stiffening from within the framework of hyperelastic models, such as Ogden models, presumably because such models are the most realistic ones available for capturing biomaterials undergoing physiologically relevant deformations [6,10]. However, such models contain multiple parameters that may be difficult to relate to any specific structure or signature.

Here we take the "minimal modeling" approach of trying to gain a theoretical understanding of compression stiffening at small strains and then test how well this linear approach does (or does not) reproduce experimental data at larger strains, fully aware that in doing so we are pushing the limits of the theory's validity. Nevertheless, our results suggest that the essential physics of compression stiffening is captured by linear elasticity theory; higher-order corrections are clearly needed at larger deformations. Thus, our interpretation of the leading-order compression stiffening mechanism is extremely simple and relies on no hyperelastic fitting parameters. We demonstrate the predictive power and universality of our approach by showing that it agrees with data from five different classes of biomaterials, including animal tissue (previously published in Refs. [5,6,10]), as well as some plant tissue and agarose gel samples, newly reported here.

That plant tissue should behave similarly to animal tissue in these prestressed rheometry experiments is not immediately obvious, given that plant cells contain cell walls, vacuoles, and chloroplasts, which animal cells do not. Plant cell walls allow the cells to withstand turgor pressures on the scale of megapascals [12] and presumably result in plant tissue typically having larger storage moduli than animal tissue at the many-cell scale. While plant tissue has long been modeled as an elastic solid [13] as has animal tissue, it is interesting to quantitatively compare the two at both small and large strain.

To provide an interpretation for the observed compressional stiffening, we point out a subtlety concerning the measurement of elastic constants of a material under prestress and argue that certain instances of linear compression stiffening can be explained by properly accounting for prestress in the rheometry experiments. The theory involved was developed in the context of condensed matter at high pressure [14] and has not commonly been applied to soft matter at physiologically relevant pressures. While prestresses in soft matter systems may be small in absolute terms, they can be large in comparison to the elastic moduli, as already mentioned. Our prestress calculation emphasizes the role of boundary conditions in determining whether the applied uniaxial stress remains uniaxial within the sample or is redistributed into an isotropic stress. Meanwhile, other instances of linear compression stiffening are not readily explained by the prestress theory. Instead, they are consistent with a conceptually different theory in which hydrostatic compression and shear are superposed on a zero-stress reference state. Thus the present work argues that *both* theories are applicable to linear compression stiffening; which one works in a given situation depends on the nature of the reference state.

II. EXPERIMENTS: MATERIALS AND METHODS

A. Animal tissue samples

The dependence of shear modulus on compressive strain has previously been reported for mouse brain [5], liver [6], and fat [10], as has the relation between axial stress and axial strain. Here we replot these data to show shear modulus as a function of axial stress. Details of the sample preparation and rheological methods are provided in Refs. [5,6,10]. Briefly, animal tissues were cut into disk-shaped samples using an 8-mm-diameter stainless steel punch. Fibrin gel, with a shear modulus greater than that of the tissues, was used to glue the sample to the rheometer plate, and a normal force of 1 g was applied to ensure contact between the top of the sample and the upper plate. This state was assumed to approximate the zero stress state. The shear modulus of the samples was measured on a strain-controlled Rheometrics fluids spectrometer III (Rheometrics, Piscataway, NJ), which can also measure normal forces simultaneously with torque. Axial strain was applied by changing the distance between the parallel plates, and the resulting axial stress was measured 30 s after changing the gap.

B. Mango samples

Mango fruit flesh was obtained from a ripe mango. Samples were cut into 10-mm-high and 20-mm-wide disks, with the long axis parallel to the seed orientation, using a 20-mm tissue punch. All samples were from the same fruit. The shear elastic and viscous modulus of mango flesh was measured using a Malvern Kinexus laboratory+ rheometer and rSpace software (Westborough, MA) using a 20-mm parallel plate geometry. Because mango is slippery, 20-mm sandpaper disks were used to ensure contact between the plates and the sample. Shear modulus was measured at 1 rad/s and 5% oscillatory strain. Triplet mango samples were measured under increasing compression, to 20% of the original sample height, in steps of 4% each.

C. Agarose gel samples

The 2% agarose solution was prepared by dispersing the appropriate amount of polymer in distilled water at 100°C, while stirring until complete dissolution. Agarose gels were prepared by pouring the above solution into a mold and allowing the gelation for 24 h at room temperature. Samples were cut from one big chunk into 9.5-, 3.8-, and 1.8-mm-high and 20-mm-wide disks using a 20-mm-tissue punch. Rheology measurements were performed using a Malvern Kinexus laboratory+ rheometer with a 20-mm parallel plate geometry. Shear modulus measurements were carried out at a frequency of 1 Hz, shear strain amplitude of 2%, and axial compressive strain increasing in steps of 5% up to maximum value 25%.

III. BARRON-KLEIN APPROACH AND PARALLEL PLATE RHEOMETRY

A. Background

A 1965 paper by Barron and Klein (hereafter BK1) treats rigorously the problem of calculating elastic constants of

a solid under prestress [15]. Taylor expanding the energy density around the prestressed reference configuration yields

$$\frac{\Delta U}{V} = S_{ij}u_{ij} + \frac{1}{2}Q_{ijkl}u_{ij}u_{kl} + \ldots, \tag{1}$$

where u_{ij} is the combined deformation due to the prestress S_{ij} and any other stresses subsequently applied to the reference state. In general, this deformation consists of a symmetric part e_{ij} and an antisymmetric part w_{ij}, i.e., $u_{ij} = e_{ij} + w_{ij}$. The key point (made 15 years prior to BK1) is that the presence of the linear term modifies the symmetry properties of the coefficients Q_{ijkl} from those of the usual rank-four elastic modulus tensor [16]. In particular, invariance of the energy density under a rigid rotation requires that

$$Q_{ijkl} - Q_{jikl} = S_{jl}\delta_{ik} - S_{il}\delta_{jk}, \tag{2}$$

$$Q_{ijkl} - Q_{ijlk} = S_{jl}\delta_{ik} - S_{jk}\delta_{il}, \tag{3}$$

$$Q_{ijkl} - Q_{jilk} = S_{jl}\delta_{ik} - S_{ik}\delta_{jl}, \tag{4}$$

where the δ's are Kronecker deltas. However, BK1 shows that there is a tensor c_{ijkl} that, in the special case of isotropic prestress $S_{ij} = -P\delta_{ij}$, where P is pressure, inherits all the symmetries of the usual elastic modulus tensor and enters the stress-strain relationship and equation of motion in the usual way. (Homogeneous deformation is assumed in their analysis.) The cost of this finite pressure generalization of the zero-stress elastic constants is that c_{ijkl} is equal to the conventional second derivative of energy density with respect to strain plus an additional "pressure correction" term, or

$$c_{ijkl} = \frac{1}{V}\frac{\partial^2 U}{\partial e_{ij}\partial e_{kl}} + \frac{P}{2}(2\delta_{ij}\delta_{kl} - \delta_{il}\delta_{jk} - \delta_{ik}\delta_{jl}). \tag{5}$$

To investigate the potential application of the BK1 approach to the compressional stiffening experiments reported here and in earlier experiments, we must consider the same deformations as in the experiments. In doing so, we study both isotropic prestress and anisotropic prestress. For the anisotropic prestress, we extend the BK1 approach.

B. Torsion with isotropic prestress

Torsional deformation of a cylinder whose axis is situated at $x = y = 0$ is equivalent to a symmetric strain

$$\begin{pmatrix} e_{xx} & e_{xy} & e_{xz} \\ e_{yx} & e_{yy} & e_{yz} \\ e_{zx} & e_{zy} & e_{zz} \end{pmatrix} = \frac{\gamma(R)}{2R}\begin{pmatrix} 0 & 0 & -y \\ 0 & 0 & x \\ -y & x & 0 \end{pmatrix}, \tag{6}$$

plus a rotation

$$\begin{pmatrix} w_{xx} & w_{xy} & w_{xz} \\ w_{yx} & w_{yy} & w_{yz} \\ w_{zx} & w_{zy} & w_{zz} \end{pmatrix} = \frac{\gamma(R)}{2R}\begin{pmatrix} 0 & -2z & -y \\ 2z & 0 & x \\ y & -x & 0 \end{pmatrix}. \tag{7}$$

Here $\gamma(r) = r\phi/L$ is the "torsional strain" which has maximum value at $r = R$ (the cylinder radius), L is the cylinder length, and ϕ is the angle of twist of one cylinder end with respect to the other [see Fig. 1(a)]. In order to apply

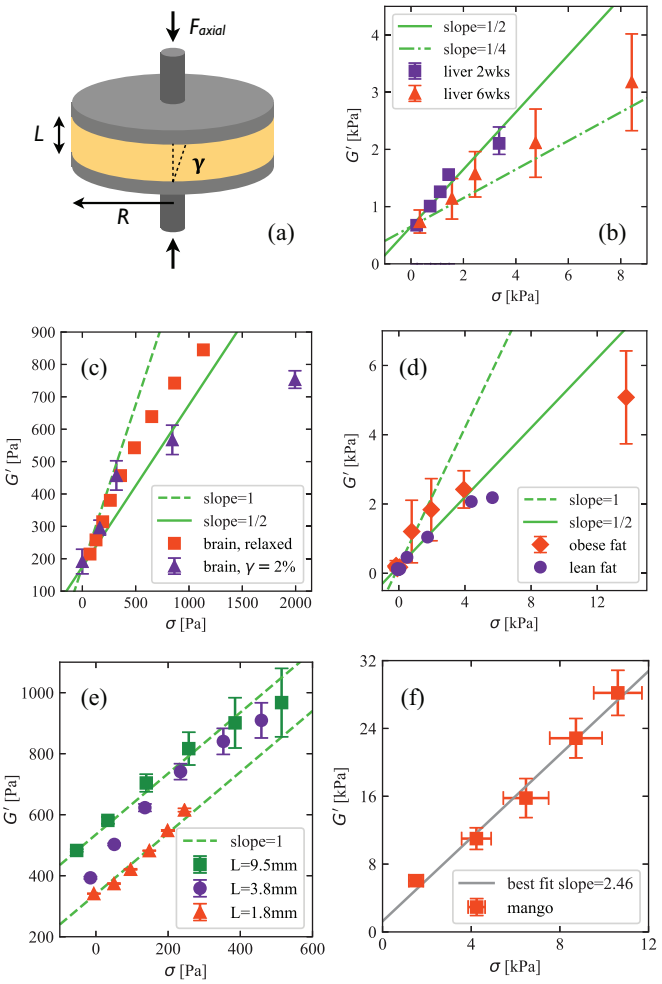

FIG. 1. (a) Schematic of rheometry experiment. In the limit $L \ll R$ and for adhesive boundary conditions, axial compression induces a volume change $\sim\pi R^2\Delta L$ [8,9]. Outside this limit, the sample is free to bulge laterally, away from a cylindrical geometry [6], and any volume change associated with the compression is $\ll \pi R^2\Delta L$. Torsion measurements were carried out at fixed axial strain $\Delta L/L$, generating axial stress deviations $\delta\sigma$ from the zero torsion prestress σ, but these were typically small, i.e., $|\delta\sigma/\sigma| \ll 1$. (b) Shear storage modulus G' versus axial compressive prestress σ for fibrotic liver tissue, 2 and 6 weeks after disease onset, replotted from Fig. 5(a) of Perepelyuk *et al.* [6]. The data points in each series correspond to axial strains of 0, 10, 15, 20, and 25%. (c) Compression stiffening data from normal mammalian brain tissue. Purple triangles are replotted from Fig. 5(c) of Pogoda *et al.* [5]. Axial strain ranges from zero to 40%, in 5 and 10% increments, respectively. (d) Compression stiffening data from the fat tissue samples studied by Mihai *et al.* [10]. Axial strain again ranges from 0 to 40% in 10% increments. (e) Compression stiffening behavior of 2% agarose gel. Different data series correspond to different sample aspect ratios (all have $R =$ 1 cm), with all three samples having been cut from the same master gel. Strain goes from 0 to 25% in 5% increments. The horizontal shifts required to collapse the $L = 9.5$ mm and $L = 3.8$ mm curves onto the $L = 1.8$ mm curve are a rough measure of the gravitational stresses present in the thicker samples—see Ref. [11]. (f) Compression stiffening behavior of mango fruit flesh, with sample aspect ratio $L/2R = 1/2$.

the BK1 formalism, we decompose the solid cylinder into small volume elements, each of which experiences a local, homogeneous strain and undergoes a rigid rotation. Consider the element located at $(x_n = r_n,\ y_n = 0,\ z_n)$ and having volume and energy V_n and U_n, respectively. The only nonzero strain component is, switching to Voigt notation, $e_4 = 2e_{yz} = 2e_{zy} = \gamma(r_n)$. Equation (5) then says that

$$c_{44} = \frac{1}{V_n}\frac{\partial^2 U_n}{\partial[\gamma(r_n)]^2} - \frac{P}{2}. \tag{8}$$

For an isotropic material with Lamé parameters $\lambda(= c_{12})$ and $\mu(= c_{44})$, this result extends to all volume elements, i.e., the shear modulus is given by

$$\mu = \frac{1}{V}\frac{\partial^2 U}{\partial \gamma^2} - \frac{P}{2}. \tag{9}$$

C. Torsion with uniaxial prestress

Next we consider the case $S_{ij} = -\sigma\delta_{iz}\delta_{jz}$. This form is perhaps easier to justify for the experiments in question, as neither redistribution of the applied stresses, nor any volume change, is assumed. Unlike the isotropically prestressed reference state, however, the current one may have transversely isotropic material symmetry (assuming the initial, unstressed material was isotropic). In other words, the cells of the tissue may be flattened in the z direction.

The counterpart to Eq. (5) is straightforwardly obtained from BK1's Eq. (4.21) for the strain energy density. We find

$$c_{ijkl} = \frac{1}{V}\frac{\partial^2 U}{\partial e_{ij}\partial e_{kl}} + \frac{\sigma}{4}(4\delta_{iz}\delta_{jz}\delta_{kl} - \delta_{iz}\delta_{kz}\delta_{jl} - \delta_{iz}\delta_{lz}\delta_{jk} - \delta_{jz}\delta_{kz}\delta_{il} - \delta_{jz}\delta_{lz}\delta_{ik}). \tag{10}$$

Caution is needed here, because while c_{ijkl} was guaranteed to be a well-defined elastic modulus tensor in the previous section, it is no longer so. There are two symmetry "violations" attributed to the uniaxial prestress, namely $c_{xxzz} - c_{zzxx} = -\sigma$ and $c_{yyzz} - c_{zzyy} = -\sigma$, according to BK1's Eq. (4.20). Fortunately, c_{44} is not directly affected by these violations and presumably remains a valid elastic constant. Proceeding under this assumption, Eq. (10) gives

$$c_{44} = \frac{1}{V}\frac{\partial^2 U}{\partial \gamma^2} - \frac{\sigma}{4} \tag{11}$$

for an isotropic or transversely isotropic material under torsion.

D. Apparent shear modulus

Suppose one disregards the prestress and defines a quantity

$$G' \equiv \frac{1}{V}\frac{\partial^2 U}{\partial \gamma^2} = \frac{\tau(R)}{\gamma(R)}. \tag{12}$$

Here the latter equality involving the maximum shear stress $\tau(R)$ is obtained by integrating the energy density $\frac{\Delta U}{V} = \frac{1}{2}G'\gamma^2(r)$ over the cylinder and comparing the result to Hooke's Law for torsion. Equation (11) now suggests that a plot of G' versus applied uniaxial prestress will be a straight line having intercept c_{44} and slope $1/4$, provided the applied uniaxial prestress remains uniaxial within the sample. But if boundary conditions, geometry, or some other factor dictates that the uniaxial prestress is redistributed into a hydrostatic pressure, slope $1/2$ is predicted [by Eq. (9)]. Intermediate slope values are predicted in the more general case where the applied compression generates a state of prestress having both uniaxial and isotropic components.

E. Analysis

In Fig. 1, we compare this predicted range of slopes (bracketed by solid and dash-dot lines) with compression stiffening data from fibrotic liver, brain, fat, agarose gel, and mango fruit flesh. With no fitting parameters, we find good agreement with fibrotic liver and reasonable agreement with lean and obese fat, but BK1 predicts too-small a rate of increase of G' for the other biomaterials. More specifically, we find that 2-week-old fibrotic liver redistributes its internal stresses isotropically, while 6-week-old fibrotic liver redistributes its internal stresses tranversely to the parallel plates. As fibrotic liver ages presumably there is more build-up of extracellular matrix (ECM) material intertwined within the cells. Perhaps such fibrous material modulates how stresses are redistributed in the presence of uniaxial compression.

Regarding fat tissue, there exists better agreement with the isotropically redistributed prestress calculation for lean fat than for obese, although for obese fat the data remain within one standard deviation of slope $1/2$ for all data points except the one at largest axial strain. Fat tissue is typically a tissue of high expandability, however, in an obese state, adipocytes become hypertrophic as a result of lipid uptake [17]. Fat tissue also contains ECM material. As fat tissue approaches the obese state, there are changes in the ECM, mainly through an increasing deposition of collagen [18].

The shear storage modulus versus axial stress for brain, agarose gel, and mango fruit flesh data do not appear to exhibit the predicted BK1 behavior. To explain these, we turn to a different theory.

IV. BIRCH APPROACH AND THE ROLE OF THE REFERENCE STATE

A. Background

Several decades prior to BK1, Birch [19] analyzed the case of hydrostatic compression superposed with shear. He assumed that for an applied stress of the form $T_{ij} = -P\delta_{ij} + T'_{ij}$, with $T'_{ij}/P \ll 1$, the strain response takes the form $e_{ij} = \epsilon\delta_{ij} + e'_{ij}$, with $e'_{ij}/\epsilon \ll 1$. The quantity T'_{ij}/e'_{ij} then defines a modulus that is amenable to analytic calculation. While there are several important differences between the Birch and BK1 treatments, the one that places them on distinct conceptual footings is the reference state, i.e., the configuration around which the energy density is expanded. Birch's moduli are valid for a zero-stress reference state, while BK1 addresses the prestressed reference state, as detailed above. Another important difference is that finite strain elasticity theory is invoked since the hydrostatic compression may be of order of the moduli of the material [19]. We will not here describe Birch's calculation in detail, because it is more complicated than BK1 and does not easily admit $P\delta_{ij} \to \sigma\delta_{iz}\delta_{jz}$ or other generalizations. Birch's result for the shear modulus of an

isotropic material is

$$G = \mu + \frac{3(3-4\nu)}{2(1+\nu)}P, \tag{13}$$

where ν is Poisson's ratio. Unlike the BK1 approach, this latter approach contains one fitting parameter in the form of Poisson's ratio. Should the material be incompressible, then there is no fitting parameter. It is illuminating that ν appears in the Birch approach but does not appear in the BK1 approach, and this contrast is at the heart of the difference between the two approaches. In BK1, all of the compression that is going to happen has already happened (to the reference state). Therefore, the material's compressibility is irrelevant to any volume conserving deformations with respect to that reference state. In Birch, the shear response is coupled to compressibility insofar as both shear and compression are applied simultaneously to the reference state.

B. Analysis

The Birch approach appears to describe those rheometry data in Fig. 1 that are not well described by BK1. In particular, the variable Poisson's ratio can generate slopes dG/dP ranging from 1 ($\nu = 1/2$) to 9/2 ($\nu = 0$) [20]. With the exception of liver and fat, the rheometry measurements reveal slopes $dG'/d\sigma$ close to 1 for nearly incompressible ($\nu \approx 1/2$) materials such as brain tissue and agarose gel. Mango tissue, like other fruit, is more compressible due to the internal structure of gas pockets [21,22], and we find that mango tissue exhibits a best-fit slope of 2.46. This value is in remarkably good agreement with Eq. (13), on substituting Poisson's ratio of mango ($\nu = 0.24 \pm 0.05$) [23], which gives $dG/dP = 2.47 \pm 0.35$. That the Birch theory should work at all for the case of applied uniaxial stress, as opposed to applied isotropic stress, is perhaps surprising. Nevertheless, the excellent agreement of Eq. (13) with mango, agarose gel, and (at small strains) brain tissue data, under $\sigma \to P$, suggests that σ is internally redistributed into a hydrostatic pressure P, even outside the thin-film limit discussed in the Introduction.

V. DISCUSSION

We extend the list of biomaterials exhibiting compressional stiffening to now include agarose gel and mango fruit flesh. The ubiquitousness of compressional stiffening in tissues calls out for an interpretative framework. By focusing on the observed (but less familiar) linear relationship between shear storage modulus and uniaxial prestress, we provide that interpretative framework via the application of two different classical elasticity results. The first is the BK1 approach, which has now been extended to the relevant experimental geometry, and the second is the Birch approach. For both approaches the shear storage modulus increases linearly with increasing axial stress and which approach applies depends on the slope of the curve. The liver and fat tissue exhibit BK1 behavior, while the agarose gel, brain, and mango tissue exhibit Birch behavior.

Materials that exhibit Birch behavior—such that applied uniaxial stress is internally redistributed as a hydrostatic pressure—appear to behave qualitatively like an elastic bag filled with fluid. This picture is suitable for both animal and plant tissue, despite the differences in cell structures, such as organelles unique to plant cells including cell walls, vacuoles, and chloroplasts. At least in principle, it should be possible to directly test for this stress redistribution by including a pressure gauge in the rheometry apparatus. Importantly, such a redistribution does not imply that the axial compression modulus observed in the rheometer experiments should be similar to the tissue bulk modulus. That may be the case in the thin-film limit, but in general, the sample is free to bulge out laterally during compression and any volume change is likely $\ll \pi R^2 \Delta L$.

The necessity of the two approaches begs the question: How can we predict which approach (i.e., reference state) is applicable for a particular sample? It is interesting to note that the liver and fat tissue contain a fibrous protein ECM, while the brain and mango tissue and agarose gel do not. Speculatively, the presence of this fibrous network could be the origin of the prestressed reference state required for BK1 behavior. Axial prestress might be generating contact changes in this network, and/or inducing anisotropies or other qualitative changes in the distribution of individual fiber tensions, such that the "composite" material's response to subsequent shear stresses is altered from what it would be in the absence of a network component. In fact, Perepelyuk *et al.* argue that the interplay of an ECM component with a cellular component is what drives compression stiffening [6]. Their proposed mechanism and conclusions are quite different from ours, as we will momentarily describe, but we do share a basic premise in that the fibrous ECM seems to play an important role in compression stiffening of liver tissue. In any case, a detailed "microscopic" understanding of BK1 and Birch's regimes of applicability to the parallel plate rheometry experiments would be an interesting direction for future work.

Given our interpretation of the compression stiffening phenomenon from within linear elasticity theory, it is interesting to consider the question of what constitutes novel compression stiffening behavior. Any elastically isotropic material (according to BK1 theory) should obey $G'(\sigma) = m\sigma + \mu$, with $1/4 \leqslant m \leqslant 1/2$ depending on boundary conditions and the material's ability to redistribute stresses, so biological tissues do not appear to be special in this regard. What *is* novel compressional stiffening behavior within the context of parallel plate rheology, we suggest, are deviations from this BK1 behavior, such as, perhaps, the Birch behavior which *requires* stress redistribution. Another type of deviation is the compression softening behavior observed in the biopolymer network materials collagen and fibrin [7,8]. Intriguingly, these also stiffen in tension, with the same magnitude of slope ($dG/d|\sigma| = 5$) as that appearing in Mears's version of the Birch theory for the appropriate Poisson ratio ($\nu = 0$) [24,25]. Yet another kind of novelty would be a transition from one slope value to another over time (given time-independent boundary conditions). As mentioned earlier, the liver tissue data in Fig. 1(b) hint at this. A possible interpretation is that some structural or compositional change occurs between 2 and 6 weeks after fibrosis onset that reduces the extent to which internal stresses are isotropically redistributed.

One prior modeling effort to interpret the observed compressional stiffening has already been mentioned. Perepelyuk *et al.* propose a phenomenological model for simultaneous description of compression stiffening, tension softening, and shear softening [6]. This model involves two components: an incompressible cellular phase and a compressible filamentous (ECM) phase. Mechanical connections between the two components are allowed to break under load and re-connect when the load is removed. Compression is thought to expel fluid through the porous ECM phase, increasing the number of cell-cell contacts and resulting in greater resistance to shear. While reasonable agreement is obtained with their liver data [replotted here in Fig. 1(b)], this agreement might be due to the fact that there are at least five fitting parameters in the model (counting the power-law exponents.) Additionally, the reliance on two components is at odds with agarose gel and with brain and mango tissue, the former lacking a cellular component and the latter lacking a filamentous component, but nonetheless exhibiting compression stiffening qualitatively similar to that of liver tissue. Meanwhile, Mihai *et al.* address compression stiffening in homogeneous materials by showing that a subclass of Ogden hyperelastic models can account for compression stiffening in brain and fat tissue [10], but again, these models have a large number of fitting parameters. In contrast, the BK1 and Birch theories provide a simple, universal explanation for compression stiffening and reasonably agree with available data spanning five different material types, the sole fit parameters being a binary choice of reference state (i.e., whether to apply BK1 or Birch), and in the case of Birch, the Poisson's ratio. For nearly incompressible materials, the latter "fit parameter" is effectively eliminated. Again, which of the two reference states is appropriate to a given sample may to be related to the presence or absence of a fibrous ECM component.

To further test the ideas herein against the models of Perepelyuk *et al.* [6] and Mihai *et al.* [10], we suggest that additional high-precision rheometer measurement be carried out for a variety of living and nonliving soft materials, with simultaneous pressure measurement and supplementary Poisson's ratio measurement, if possible. Also, since in the BK1 theory it is c_{44}, not G', that appears in the equation of motion and determines the speed of transverse sound $v_t = \sqrt{c_{44}/\rho}$, an independent measurement of sound velocity could constrain c_{44} and verify that any pressure dependence of v_t enters only through the equation of state, $\rho(P)$, where ρ is density. Finally, we mention that in the context of tumor identification and visualization, the distinction between c_{44} and G' should be important for certain types of ultrasound imaging, especially shear wave elastography [26].

ACKNOWLEDGMENTS

T.A.E. wishes to thank Daniel Sussman for providing some useful references. T.A.E. and J.M.S. acknowledge financial support from NSF-DMR-CMMT Award No. 1507938. K.P., K.C., and P.A.J. acknowledge financial support from NSF DMR 17-20530 and NIH GM096971.

[1] M. Basan, T. Risler, J.-F. Joanny, X. Sastre-Garau, and J. Prost, HFSP J. **3**, 265 (2009).
[2] J. Weickenmeier, R. de Rooij, S. Budday, P. Steinmann, T. C. Ovaert, and E. Kuhl, Acta Biomater. **42**, 265 (2016).
[3] S. Budday, G. Sommer, C. Birkl, C. Langkammer, J. Haybaeck, J. Kohnert, M. Bauer, F. Paulsen, P. Steinmann, E. Kuhl, and G. A. Holzapfel, Acta Biomater. **48**, 319 (2017).
[4] A. Arani *et al.*, Mag. Res. Med. **79**, 1043 (2018).
[5] K. Pogoda, L. Chin, P. C. Georges, F. J. Byfield, R. Bucki, R. Kim, M. Weaver, R. G. Wells, C. Marcinkiewicz, and P. A. Janmey, New J. Phys. **16**, 075002 (2014).
[6] M. Perepelyuk, L. Chin, X. Cao, A. van Oosten, V. B. Shenoy, P. A. Janmey, and R. G. Wells, PLoS ONE **11**, e0146588 (2016).
[7] A. J. Licup, S. Münster, A. Sharma, M. Sheinman, L. M. Jawerth, B. Fabry, D. A. Weitz, and F. C. MacKintosh, Proc. Natl. Acad. Sci. USA **112**, 9573 (2015).
[8] M. Vahabi, A. Sharma, A. J. Licup, A. S. G. van Oosten, P. A. Galie, P. A. Janmey, and F. C. MacKintosh, Soft Matt. **12**, 5050 (2016).
[9] A. S. G. van Oosten, M. Vahabi, A. J. Licup, A. Sharma, P. A. Galie, F. C. MacKintosh, and P. A. Janmey, Sci. Rep. **6**, 19270 (2016).
[10] L. A. Mihai, L. Chin, P. A. Janmey, and A. Goriely, J. R. Soc. Interface **12**, 20150486 (2015).
[11] Adhesive contact also provides a means of reducing stresses generated by the sample's own weight; for 5-mm cubes of brain tissue, the associated gravitational strains can apparently be as large as 60% [3], an order of magnitude larger than one expects based on a simple calculation.
[12] P. Schopfer, Am. J. Bot. **93**, 1415 (2006).
[13] P. Ghysels, G. Samaey, B. Tijskens, P. V. Liedekerke, H. Ramon, and D. Roose, Phys. Biol. **6**, 016009 (2009).
[14] G. Grimvall, B. Magyari-Köpe, V. Ozoliņš, and K. A. Persson, Rev. Mod. Phys. **84**, 945 (2012).
[15] T. H. K. Barron and M. L. Klein, Proc. Phys. Soc. **85**, 523 (1965).
[16] K. Huang, Proc. Roy. Soc. A **203**, 178 (1950).
[17] K. Sun, C. M. Kusminski, and P. E. Scherer, J. Clin. Invest. **121**, 2094 (2011).
[18] N. Alkhouli *et al.*, Am. J. Physiol. Endocr. Metab. **305**, E1427 (2013).
[19] F. Birch, J. Appl. Phys. **9**, 279 (1938).
[20] It is worth noting that Mears *et al.* construct a shear modulus from Birch's result for Young's modulus, obtaining a result similar to, but not identical to, Eq. (13). In their version, dG/dP ranges from 1 to 5 [24,25].

[21] Q. T. Ho, P. Verboven, H. K. Mebatsion, B. E. Verlinden, S. Vandewalle, and B. M. Nicolaï, New Phytol. **182**, 163 (2009).
[22] M. Grotte, F. Duprat, E. Piétri, and D. Loonis, Int. J. Food Prop. **5**, 333 (2002).
[23] B. Jarimopas, P. Sirisomboon, R. Sothornwit, and A. Terdwongworakul, in *Focus on Food Engineering Research and Developments*, edited by V. N. Pletney (Nova Publishers, New York, 2007), p. 239.
[24] D. R. Mears, K. D. Pae, and J. A. Sauer, J. Appl. Phys. **40**, 4229 (1969).
[25] E. J. Parry and D. Tabor, J. Mater. Sci. **9**, 289 (1974).
[26] A. P. Sarvazyan, O. V. Rudenko, S. D. Swanson, J. B. Fowlkes, and S. Y. Emelianov, Ultrasound Med. Biol. **24**, 1419 (1998).